35th Annual International Conference of the IEEE EMBS
Osaka, Japan, 3 - 7 July, 2013

An Extended Model of Blood Pressure Variability: Incorporating the Respiratory Modulation of Vascular Resistance

Patjanaporn Chalacheva, *Student Member, IEEE* and Michael C.K. Khoo, *Fellow, IEEE*

Abstract— **Short-term blood pressure variability is generally attributed to the baroreflex feedback control on heart rate and systemic vascular resistance (SVR), and the mechanical effect of respiration on stroke volume. Although it is known that respiration affects sympathetic outflow and deep breaths can lead to peripheral vasoconstriction, the respiratory modulation of SVR has been little studied. In the present study, we investigated the dynamics resulting from the respiratory modulation of SVR and its effect on blood pressure variability by employing structured and minimal modeling approaches. Using peripheral arterial tonometry as a noninvasive measure of SVR, we were able to estimate the respiratory-vascular conductance coupling mechanism. We found that the dynamics of the sigh-vasoconstriction reflex could be reproduced only when the respiratory modulation of SVR was incorporated into the closed-loop model. Lastly, we demonstrated that taking this respiratory modulation effect into account is essential for accurately estimating the dynamics of the SVR baroreflex.**

I. Introduction

The spontaneous variabilities observed in measurements of heart rate (HR) and arterial blood pressure (ABP) reflect the dynamic behavior of regulatory mechanisms, such as the baroreflexes and chemoreflexes, as they interact with perturbations that originate from external sources or other organ systems [1]. It is now well known that heart-rate variability can be attributed to the underlying dynamics that result from three major mechanisms. HR fluctuations that are correlated with respiration ("respiratory sinus arrhythmia", RSA) result from direct coupling between respiratory and cardiovagal neurons in the medullary structures as well as vagal feedback from the pulmonary stretch receptors. HR oscillations of both the low-frequency (0.04-0.15 Hz) and high-frequency (0.15-0.4 Hz) varieties can also be generated by fluctuations in ABP via the baroreceptors. In turn, HR fluctuations and the mechanical modulation of stroke volume by respiration contribute to blood pressure variability. Baroreflex control of peripheral vascular tone also plays an important role in generating blood pressure variability.

It is well established from measurements of peroneal nerve activity that respiration modulates sympathetic neural outflow [2]. However, it appears that the respiratory-related oscillations in sympathetic activity exert a strong modulatory influence on peripheral vascular tone only at lower frequencies [3]. Previous studies have shown rather consistently that deep breaths, akin to sighs, trigger peripheral vasoconstriction response [4, 5]. Similarly, we have observed this sigh-vasoconstriction response through measurements using peripheral arterial tonometry (PAT) or laser Doppler flow monitoring. PAT employs the principles of plethysmography to capture pulsatile volume changes in the finger produced by vasoconstriction or vasodilation [6]. Reductions/increases in amplitude of the PAT signal provide quantitative measures of vasoconstriction/vasodilation.

Existing cardiovascular control models provide characterizations at various levels of detail of the closed-loop dynamics that underlie HR and ABP variability. However, to our knowledge, none has included the effect of respiration on peripheral vascular tone. The objective of this study is to develop an extended model of blood pressure variability that adequately captures the dynamics resulting from the respiratory modulation of systemic vascular resistance (SVR). This is accomplished through a combination of structured and minimal modeling approaches. We further show that taking this effect into account is important for obtaining accurate estimates of the dynamics that characterize the baroreflex control of SVR.

II. Methods

A. Structured Model

The starting point of this study is the structured model (A) shown schematically in Fig. 1. Using a simple 2-element Windkessel model, the model generates a pulsatile waveform of ABP for each cardiac cycle. Respiration, represented by instantaneous lung volume (ILV), modulates ABP indirectly through its effect on heart rate (via the RSA mechanism). Through changes in intrathoracic pressure, respiration produces mechanically-induced alterations in stroke volume which in turn lead to fluctuations in ABP. This mechanical effect of respiration (MER) is modeled as a derivative of ILV multiplied by a negative gain [7]. The final ABP, which contains these influences combined, then becomes the input to the model components that represent baroreflex control of HR and SVR. For greater consistency of comparison with our experimental results that were derived from PAT measurements, we will quantify SVR by its inverse: systemic vascular conductance (SVC = 1/SVR).

The baroreflex control of SVR is modeled as a nonlinear negative static gain [8] connected to a time delay of 5 seconds [8] and a lowpass filter. The dynamically changing SVR output is fed into the Windkessel model in order to represent beat-by-beat changes in the time constant of the

This work was supported in part by U.S. National Institute of Health grant P41-EB001978.

P. Chalacheva is with the Biomedical Engineering Department, University of Southern California, Los Angeles, CA 90089 USA (phone: 213-740-0827; fax: 213-821-3897; e-mail: chalache@usc.edu).

M. C.K. Khoo is with the Biomedical Engineering Department, University of Southern California, Los Angeles, CA 90089 USA (e-mail: khoo@bmsr.usc.edu).

Windkessel. The baroreflex control of HR is divided into 2 branches: sympathetic and parasympathetic control. Each of these branches is modeled as a nonlinear static gain [8]. The output of each of these branches is combined with the RSA effect on HR [7]. The RSA is modeled as a constant gain that increased HR during inspiration and decreased HR during expiration. The combined HR output is used as the input to the sinoatrial (SA) node.

The dynamics of the SA node are divided into sympathetic and parasympathetic components. Both branches are modeled as lowpass filters with constant gains [7]. In addition, a time delay of 1.7 seconds [7] is added to the sympathetic branch to mimic latency in the sympathetic response. The outputs from each branch in the SA node are combined to obtain the final HR. This HR then enters the "properties of myocardium" block, which represents the influence of the duration of pulse interval on stroke volume. A longer pulse interval would lead to an increase in the next stroke volume and thus pulse pressure (PP) [9]. The new PP is then fed into the Windkessel model for generation of the next cardiac cycle.

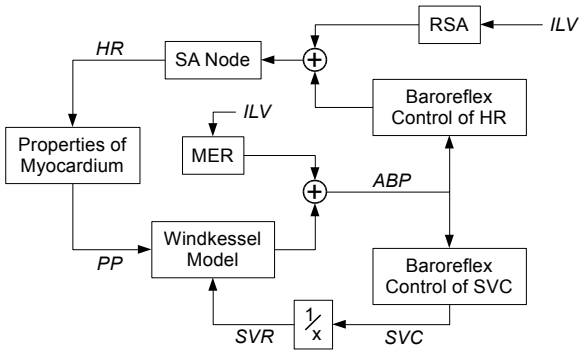

Figure 1. Simulation Model A

B. Minimal Model

A minimal modeling approach is employed for quantifying the effect of respiration on SVC using experimental data. The database consists of short-term recordings of ILV, RRI, MAP and PAT measured in 10 human subjects in the supine posture. The amplitude of the PAT signal is used to represent changes in SVC.

We propose two hypotheses: 1) fluctuations in SVC due to respiration are produced by respiratory-modulated ABP and 2) in addition to ABP, respiration also directly produces fluctuations in SVC. Based on the first hypothesis, the fluctuations in SVC (ΔSVC) can be modeled as a one-input model, relating fluctuations in beat-averaged ABP (ΔMAP) to ΔSVC through a baroreflex control of vascular conductance (BVC). The mathematical representation of the one-input model is

$$\Delta SVC(t) = \sum_{i=0}^{M-1} h_{BVC}(i)\Delta MAP(t-i-T_{BVC}) + \varepsilon_{SVC}(t). \quad (1)$$

The second hypothesis, however, requires 2 dynamic components to characterize ΔSVC. The first component is the BVC and the second component represents respiratory-vascular conductance coupling (RVC), relating changes in ILV (ΔILV) to ΔSVC.

$$\Delta SVC(t) = \sum_{i=0}^{M-1} h_{BVC}(i)\Delta MAP(t-i-T_{BVC}) + \sum_{i=0}^{M-1} h_{RVC}(i)\Delta ILV(t-i-T_{RVC}) + \varepsilon_{SVC}(t). \quad (2)$$

In both cases, PAT amplitude is employed as a measure of SVC. h_{BVC} and h_{RVC} represent the impulse responses of BVC and RVC, respectively; T_{BVC} and T_{RVC} represent the time delays of BVC and RVC, respectively; M represents the memory of the system; and ε_{SVC} represents other fluctuations in SVC that cannot be explained by the model. Both minimal models are assumed to be linear and time-invariant. Therefore, complete characterization of BVC and RVC can be accomplished by identifying the impulse responses. To estimate an impulse response, we employ a kernel expansion technique as it greatly reduces the number of parameters to be estimated. Meixner functions are employed as the basis functions such that each impulse response can be represented as a weighted sum of the Meixner basis functions (MBF) [9]. Each impulse response is assumed to have duration of 30 sampling intervals (i.e. M=30) where each sampling interval is 0.5 seconds. Using this technique, each impulse response is represented as

$$h(t) = \sum_{j=1}^{q} c_j B_j^{(n)}(t) \quad (3)$$

where $B_j^{(n)}(t)$ are the orthonormal set of MBF with n^{th} order of generalization. The larger the value of n, the longer it takes for the MBF to reach their maximum values. The coefficients, c_j, represent the weights of $B_j^{(n)}(t)$. q represents the total number of MBF used in the expansion of the impulse response.

Using (3), we can rearrange (1) and (2) such that ΔSVC is equal to the summation of the expansion coefficient times the convolution of the MBF with the inputs [10]. The unknown expansion coefficients c_j^{BVC} and c_j^{RVC} can be estimated using least-squares minimization. The least-squares minimization process is repeated for a range of values of delays (T_{BVC} from 2 to 8 seconds and T_{RVC} from 0 to 6 seconds), the order of generalization (n from 0 to 5), and the Meixner function order (q_{BVC} and q_{RVC} from 2 to 8). For each combination of the model parameters, the minimum description length (MDL) [11] is employed as a measure of the quality of data fitting.

$$MDL = \log(J_R) + \frac{total\ no.\ of\ parameters \times \log(M)}{M} \quad (4)$$

J_R is the variance of the residual errors between the measured and the predicted output. The total number of parameters is the total number of unknown coefficients needed to be estimated. The optimal set of parameters is selected based on the global search for minimal MDL. Once the expansion coefficients are computed, the impulse response can then be obtained using (3).

C. *Incorporating RVC into the Simulation Model*

The sigh-vasoconstriction block is incorporated into the simulation model A (Fig. 1). This block consists of a constant gain and a representative RVC impulse response obtained from the two-input minimal model. ILV is the input of the sigh-vasoconstriction block and its output, ΔSVR due to changes in ILV, is obtained by convolving RVC impulse response with ILV. This output is added to the output of the baroreflex control of SVC block to obtain a total SVC. The total SVC is then inverted to SVR before being fed into the Windkessel model. The extended simulation model (B) is shown in Fig. 2.

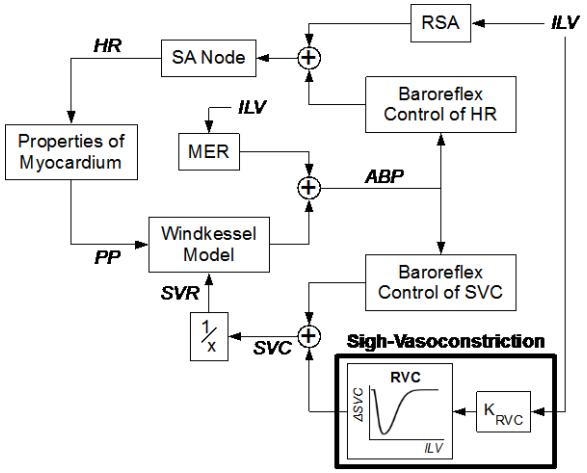

Figure 2. Simulation Model B

III. RESULTS

Predictions from the simulation model A and B are compared to the experimental data of one subject in Fig. 3. Simulation model A shows that RRI shortened during the sigh due to the RSA mechanism. Consequently, MAP increases in response to the reduction in RRI. This increase in MAP in turn causes the lengthening in RRI through baroreflex control of HR. Also, approximately 5 seconds after the initiation of the sigh, SVC increases, indicating vasodilation response. Model A is able to reproduce all the effects that are included in the model as expected and is able to mimick some features of the response observed in the experimental data. However, one obvious discrepancy between the simulated output from the Model A and the experimental data is the SVC response. While the experimental data show a transient vasoconstriction following the sigh, Model A, however, predicts a vasodilation response.

The sigh-vasoconstriction response, as characterized by the RVC impulse response, is estimated from the experimental data in an open-loop manner as described in Section B. A representative RVC impulse response (Fig.4) derived from application of the minimal model to 10 sets of human data is incorporated into the sigh-vasoconstriction block of Model B. With the simulation model operating in a closed-loop fashion, model B demonstrates the ability to simulate the patterns of cardiovascular variability observed in real data, including the sigh-vasoconstriction response as shown in Fig. 3 (right panel).

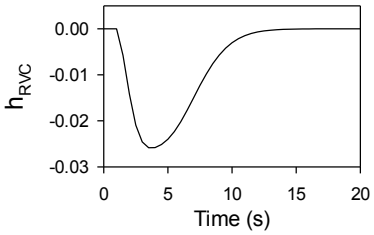

Figure 4. Representative RVC impulse response

Fig. 5 illustrates normalized power spectra of the sigh data segments from the experimental data obtained from one subject, and from simulation Models A and B. The power spectra show that RRI, MAP, and SVC from both experimental data and simulation models exhibit oscillations at the respiratory frequency. RRI, in particular, shows strong coupling with respiration. In addition, these signals also

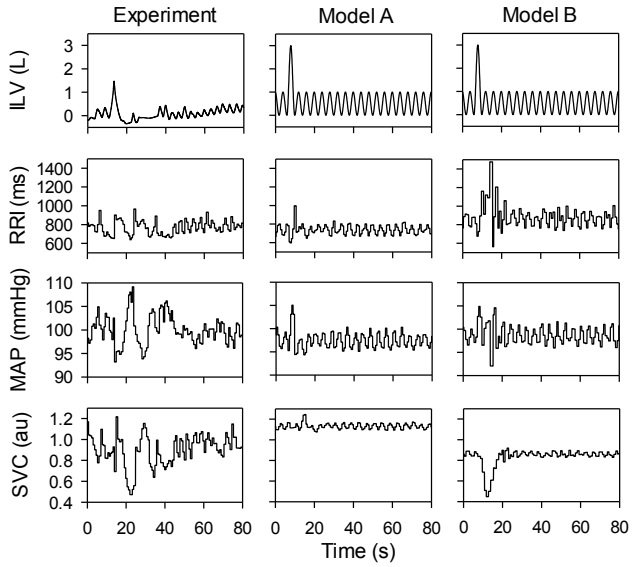

Figure 3. Data segments during a sigh from the experimental data (left panel) compared with simulation outputs of Model A (middle panel), and Model B (right panel).

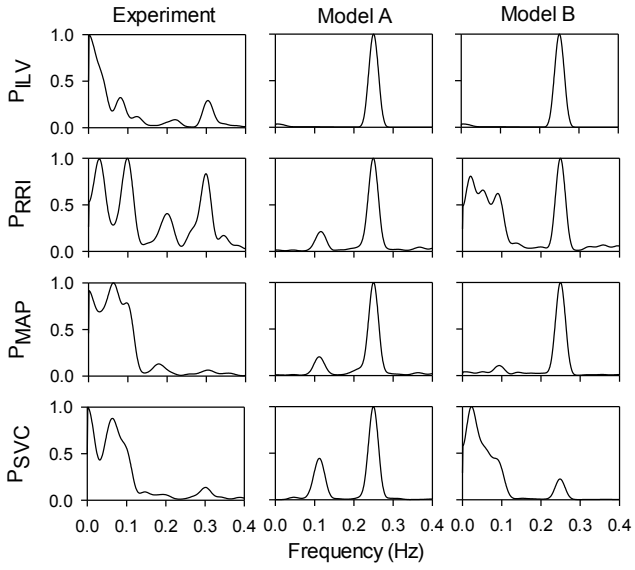

Figure 5. Normalized power spectra of the data segments during a sigh from the experimental data (left panel), the simulation model A (middle panel), and the simulation model B (right panel).

exhibit low-frequency oscillations at around 0.1 Hz. MAP and SVC shows prominent low-frequency components compared to the power at the respiratory frequency. All power spectra of the simulated signals from the Model A exhibit pronounced respiratory frequency component. The MAP power spectra from both simulation models show much more prominent peaks at the respiratory frequency compared to the lower frequencies, in contrast to the power spectrum of MAP obtained from the experiment. This is likely due to other influences on MAP not captured by the rather simple simulation models. However, the SVC power spectrum of the Model B is more similar to that of the experimental data in exhibiting a more prominent low-frequency component relative to the respiratory frequency component.

The one-input minimal model is applied to the data generated from the simulation model B. We find that although the model prediction fits the actual output reasonably well, the estimated h_{BVC} using the one-input model shows an opposite response to the "true" h_{BVC}, the impulse response of BVC in the simulation model B (Fig. 6).

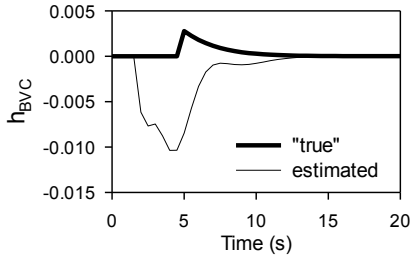

Figure 6. Estimated h_{BVC} from data generated by simulation model B using one-input minimal model

IV. Discussion

In the present study, we have employed a combination of structured and minimal modeling approaches to develop a closed-loop model of blood pressure variability that would adequately capture the dynamics resulting from the respiratory modulation of SVR. In particular, we were able to accurately predict the dynamics of the sigh-vasoconstriction reflex only after incorporating the RVC component into the model. Furthermore, since RVC tends to generate an opposite response to BVC, it is important to take into account of the respiratory modulation of SVR in order to obtain an accurate estimation of BVC. Otherwise, the estimated BVC can appear to exhibit an opposite response to what is generally expected. We have confirmed this result in further work not presented here due to limitations of space.

Although this simulation model developed in this study is able to reproduce the responses similar to what would be expected in a physiological system under normal conditions, it does not include the effects of other regulatory influences that also contribute to short-term blood pressure variability, such as local vascular factors, cardiopulmonary reflexes, chemoreflexes, and the effects of breath-to-breath variability in respiratory tidal volume and breath period. The dominating peak at the respiratory frequency in the simulated MAP (Fig. 5) suggests that the relative contributions of the RSA mechanism and the respiratory modulation of stroke volume in Model B to the fluctuations in MAP may have been overly weighted in our simulations.

Another point that should be addressed is the use of the amplitude of PAT signal as a measure of SVC. In this study, PAT has shown to be a useful device in detecting the vasoconstriction response. However, it does not directly measure SVR but rather the changes in the blood volume at the fingertip. The changes in SVR are then inferred from the changes in volume but whether the relationship between SVR and amplitude of PAT is linear or not has yet to be determined. In addition, PAT provides only ***relative*** measurements of vasoconstriction in the finger; this complicates comparisons of PAT measurements across subjects.

V. Conclusions

The respiratory modulation of SVR is an important mechanism that contributes to blood pressure variability. Moreover, taking this respiratory modulation effect into account is essential for accurately estimating the dynamics of the baroreflex control of SVR.

References

[1] G. Parati, G. Mancia, M. Di Rienzo, and P. Castiglioni, "Point: cardiovascular variability is/is not an index of autonomic control of circulation," *J Appl Physiol,* vol. 101, no. 2, pp. 676-8; discussion 681-2, Aug, 2006.

[2] D. L. Eckberg, "Respiratory Sinus Arrhythmia and Other Human Cardiovascular Neural Periodicities," *Regulation of Breathing*, Lung Biology in Health and Disease J. A. Dempsey and A. I. Pack, eds., pp. 669-740, New York: Marcel Dekker, 1995.

[3] S. C. Malpas, B. L. Leonard, S. J. Guild, J. V. Ringwood, M. Navakatikyan, P. C. Austin, G. A. Head, and D. E. Burgess, "The sympathetic nervous system's role in regulating blood pressure variability," *IEEE Eng Med Biol Mag,* vol. 20, no. 2, pp. 17-24, Mar-Apr, 2001.

[4] B. Bolton, E. A. Carmichael, and G. Sturup, "Vaso-constriction following deep inspiration," *J Physiol,* vol. 86, no. 1, pp. 83-94, Jan 15, 1936.

[5] S. Sangkatumvong, M. C. Khoo, R. Kato, J. A. Detterich, A. Bush, T. G. Keens, H. J. Meiselman, J. C. Wood, and T. D. Coates, "Peripheral vasoconstriction and abnormal parasympathetic response to sighs and transient hypoxia in sickle cell disease," *Am J Respir Crit Care Med,* vol. 184, no. 4, pp. 474-81, Aug 15, 2011.

[6] D. A. Goor, J. Sheffy, R. P. Schnall, A. Arditti, A. Caspi, E. E. Bragdon, and D. S. Sheps, "Peripheral arterial tonometry: a diagnostic method for detection of myocardial ischemia induced during mental stress tests: a pilot study," *Clin Cardiol,* vol. 27, no. 3, pp. 137-41, Mar, 2004.

[7] J. P. Saul, R. D. Berger, P. Albrecht, S. P. Stein, M. H. Chen, and R. J. Cohen, "Transfer function analysis of the circulation: unique insights into cardiovascular regulation," *Am J Physiol,* vol. 261, no. 4 Pt 2, pp. H1231-45, Oct, 1991.

[8] J. B. Madwed, P. Albrecht, R. G. Mark, and R. J. Cohen, "Low-frequency oscillations in arterial pressure and heart rate: a simple computer model," *Am J Physiol,* vol. 256, no. 6 Pt 2, pp. H1573-9, Jun, 1989.

[9] R. W. deBoer, J. M. Karemaker, and J. Strackee, "Hemodynamic fluctuations and baroreflex sensitivity in humans: a beat-to-beat model," *Am J Physiol,* vol. 253, no. 3 Pt 2, pp. H680-9, Sep, 1987.

[10] V. Belozeroff, R. B. Berry, C. S. Sassoon, and M. C. Khoo, "Effects of CPAP therapy on cardiovascular variability in obstructive sleep apnea: a closed-loop analysis," *Am J Physiol Heart Circ Physiol,* vol. 282, no. 1, pp. H110-21, Jan, 2002.

[11] J. Rissanen, "Estimation of structure by minimum description length," *Circ Syst Sig Process,* vol. 1, pp. 395-406, 1982.